J Mater Sci: Mater Electron (2016) 27:10791–10797
DOI 10.1007/s10854-016-5184-z

Synthesis, structural, and electrical characterization of RuO_2 sol–gel spin-coating nano-films

G. Lakshminarayana[1,2,3] · I. V. Kityk[4] · T. Nagao[1,2,5]

Received: 21 April 2016 / Accepted: 11 June 2016 / Published online: 20 June 2016

Abstract In this work a series of RuO_2 thin films were synthesized through sol–gel spin coating processes and their structural and electrical properties are studied. The (1 1 0), (1 0 1), (2 0 0), and (2 1 1) characteristic peaks of RuO_2 phase are identified from the annealed RuO_2 films X-ray diffraction profiles. Through the Atomic Force Microscopy, the surface roughness values of the films evaluated as 1.2 nm, and 0.9 nm for 0.5, and 1.0 mmol RuO_2 films, respectively. With Ru molar ratio increment the optical transparency of the synthesized films decreases in the UV–Vis-IR range. The P-type conductivity of RuO_2 film is confirmed by Hall Effect measurement and the resistivity of 1.0 mmol RuO_2 film annealed at 600 °C acquired by Hall measurement was 2.9×10^{-4} Ω cm. The synthesized RuO_2 nano-thin films characterization demonstrates that an optically transparent conductive material can be reliably and efficiently created using simple sol–gel spin-coating methods.

✉ G. Lakshminarayana
glnphysics@gmail.com

✉ I. V. Kityk
iwank74@gmail.com

1 International Center for Materials Nanoarchitectonics (MANA), National Institute for Materials Science, 1-1 Namiki, Tsukuba 305-0044, Japan

2 CREST, Japan Science and Technology Agency, 4-1-8 Honcho, Kawaguchi, Saitama 332-0012, Japan

3 Wireless and Photonic Networks Research Centre, Faculty of Engineering, Universiti Putra Malaysia, 43400 UPM Serdang, Selangor, Malaysia

4 Faculty of Electrical Engineering, Czestochowa University of Technology, Armii Krajowej 17, 42-201 Czestochowa, Poland

5 Department of Condensed Matter Physics, Graduate School of Science, Hokkaido University, Kita-10 Nishi-8 Kita-ku, Sapporo 060-0810, Japan

1 Introduction

Ruthenium dioxide, RuO_2, is a conductive ceramics that belongs to the family of transition metal oxides with tetragonal rutile-type structure. Among many other conductive oxides, RuO_2 exhibits distinct physical and chemical properties and has been used in various applications such as diffusion barriers [1], thin-film resistors [2], bottom electrodes of ferroelectric thin films in dynamic random access memories (DRAMs) [3], and electrochemical capacitors [4]. As one of the most promising electronic ceramics, nano-scale films of RuO_2 can be used for a wide variety of applications because of its semi-metallic conductivity (i.e., 35 μΩ cm: bulk single crystal) as well as good thermal stability [5], excellent diffusion barrier properties [6, 7], and high chemical corrosion resistance [8–10]. One of the most promising and important use of RuO_2 is for the applications in organic light emitting devices (OLED), flat panel display and organic solar cells. This is because the ultrathin films of RuO_2 are transparent and has high enough work function (5.2 eV) which realizes excellent hole conduction into the active layer of the device. The primary requirement here is the sufficiently high electrical conductance, high optical transparency, and smoothness as well as the closed nature of the film to avoid current leakage in the fabricated devices that also promotes smooth growth of the organic layers. Especially the latter two features are of particular importance to make low-wattage high-performance light emitting device or flat panel displays.

Up to now, most of the reported RuO_2 thin films are prepared by physical vapor deposition (PVD) and

subsequent oxidation of Ru films, or by direct deposition of RuO_2 by magnetron sputtering [11], or reactive sputtering of Ru [12]. More recently, metal organic chemical vapor deposition (MOCVD) [13, 14], pulsed laser deposition (PLD) [15], electrodeposition from aqueous solution [16] or cyclo voltammetry [17], atomic layer deposition (ALD) [18], and chemical vapor deposition(CVD) [19], are also used for the fabrication of RuO_2 films. Polycrystalline RuO_2 thin films have been routinely deposited on different substrates by the techniques mentioned above. However, a serious drawback in the processing of materials based on RuO_2 is the well-established chemical reactivity above $\sim$700 °C where RuO_2 becomes volatile and oxidizes to RuO_3/RuO_4 gases (in air) or reduces to Ru metal (in a vacuum) [20].

Compared with commonly used vacuum-based techniques, the sol–gel method is a low- temperature "soft" synthesis process which is relatively simple and cost effective method. This method allows a soft chemical tailoring of the composition and texture of the final product by a suitable choice of the synthesis conditions and of the starting precursors [21]. The sol–gel method is often adopted with spin coating and subsequent mild annealing to yield uniform nano-scale layer across the substrate surface [22, 23]. The film thickness can be controlled by the rotational frequency and accurate controlling of the films thickness can be done. However, up to date, there are very few reports yet available in the literature for the synthesis of RuO_2 thin films by using the sol–gel process [21, 24].

In the present work we report on the sol–gel synthesis of smooth ultrathin films of RuO_2 with precisely controlled thickness in the nanometer region. The films were wet-chemically synthesized and coated through sol–gel spin coating processes. Subsequently their crystal structure, surface morphology, thickness, roughness, optical transmittance, functional groups, electrical resistivity, carrier concentration, and mobility are studied. The fabricated film showed good electrical transport and high optical transparency together with high surface smoothness suitable for the use in organic electronics. The fabrication method reported here can open a way to readily fabricate smooth and optically transparent conductive nano-films with cost effective and relatively mild synthesis route, which fits nicely to the application for organic optoelectronics as well as for solar energy harvesting devices.

2 Experimental

2.1 Synthesis

It was reported that [21], RuO_2–SiO_2 nano-composite films were obtained by dip-coating from alcoholic solutions of $Ru(OEt)_3$ and subsequent thermal treatments in air or N_2 between 100 and 400 °C, and mixed RuO_2–SiO_2 coatings were synthesized starting from solutions of $RuCl_3$ and $[NH_2(CH_2)_2NH(CH_2)_3Si(OMe)_3]$. The choice of suitable precursors and moderate temperature processing has proved to be effective to obtain RuO_2–based nanostructured coatings, whose purity increased with the annealing temperature from 100 to 400 °C [21]. Following the Ref. [24], ruthenium oxide films were prepared by sol–gel spin coating technique using aqueous solution of ruthenium (III)-nitrosylnitrate $Ru(NO)(NO_3)_3$ in 2-methoxyethanol and typical film thicknesses achieved are several 100 nm after calcinations at 1000 K for 2 h with high crystallinity. In this work, we have synthesized three RuO_2 thin films using sol solutions with Ru concentrations of 0.25, 0.5, and 1.0 mmol; spin coated on both p type Si (1 0 0) substrates and silica glass substrates. For RuO_2 sol solution (light to deep purple), stoichiometric amounts of $RuCl_3{\cdot}nH_2O$ (Wako Chem. Com., Japan; we speculated "n" should be 3.5 here) were first mixed with 10 ml absolute ethanol (Wako Chem. Com., Japan), and then stirred with a magnetic stirrer for 2 h at room temperature. The sols were allowed to age for a minimum of 48 h in a sealed container prior to spin coating. After spin coating (conditions: 3000 rpm/30 s. with 50 µl solution) on the substrates, the films were dried at 60 °C for 12 h under vacuum. Finally, the films were annealed in vacuum (c.a.1 mm Hg) in a horizontal quartz-tube furnace at 400, 450, 500, 600, and 700 °C for 30 min.

2.2 Characterization

The X-ray diffraction (XRD) profiles were obtained on a Rigaku X-ray diffractometer (model Rint 2000) with Cu–K_α ($\lambda = 1.542$ Å) radiation using an applied voltage of 40 kV and 40 mA anode current, calibrated with Si at a rate of 2 deg/min. The surface morphology of the prepared samples was observed by scanning electron microscopy (SEM; S-4800 HITACHI Company) at 1 nm resolution and an acceleration voltage of 5 kV. The surface morphology and texture of the deposited RuO_2 films was also measured using atomic force microscopy (AFM) (SII E-Sweep) using tapping mode. Si cantilever (SI-DF20) with spring constant of 14 N/m and frequency of 134 kHz was used. The Fourier transform infrared (FTIR) spectra of the thin films were measured in the transmission mode over the 100–6000 cm^{-1} range by a Thermo Nicolet NEXUS-670 FTIR machine using solid substrate beam splitter and DTGS polyethylene detector with a spectral resolution of $\sim$4 cm^{-1}. The optical transmission spectra of the thin films coated on glass substrates were measured by using JASCO V-7200 absorption spectrophotometer in the range 300–3500 nm. The mobility and carrier concentration of

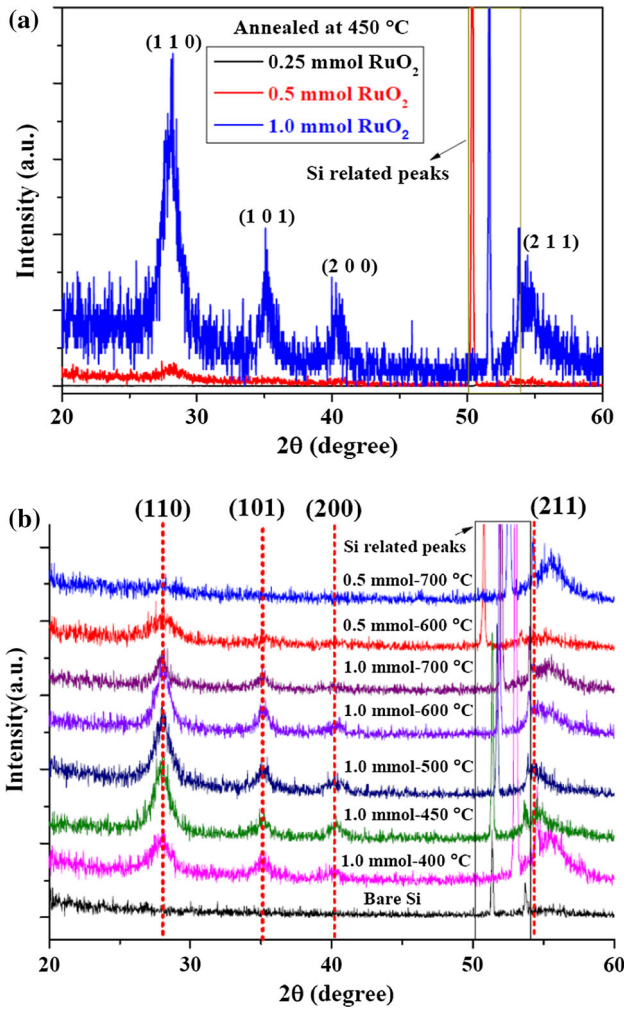

Fig. 1 XRD profiles of the RuO_2 films annealed at **a** 450 °C, **b** at different temperatures

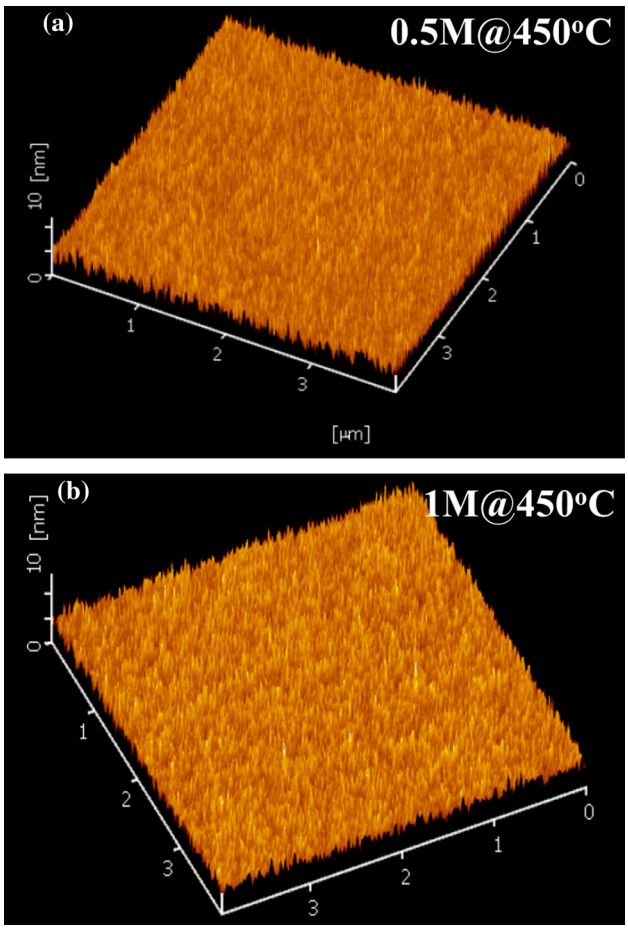

Fig. 2 AFM images of **a** 0.5 mmol, and **b** 1.0 mmol RuO_2 films annealed at 450 °C

the fabricated RuO_2 nano-films were examined by using a Hall measurement system (Model 8403 AC/DC Hall Effect Measurement System, Toyo Corporation) based on the Van der Pauw four-probe technique, at room temperature in air.

3 Results and discussion

This work is aimed at obtaining smooth and ultrathin coatings of pure RuO_2 on Silicon and glass substrates with controlled uniformity in both morphology and chemical composition. We examined the SEM images (not shown here) of the as-coated and dried at 60 °C thin films. Before annealing, the RuO_2 films of various compositions all exhibited smooth and continuous morphology when observed by SEM. To determine the phases present in the samples after annealing at 400–700 °C, we analyzed the samples by XRD. Figure 1a, b show the XRD patterns of the RuO_2 films annealed at 450 °C and 0.5, and 1.0 mmol RuO_2 films at different annealing temperatures. From Fig. 1 one can observe that after annealing, diffraction peaks of the RuO_2 phase are present (i.e., RuO_2 phase precipitates.) in the samples of 0.5 mmol annealed at 450, 600 and 700 °C including for 1.0 mmol RuO_2 annealed at 400–700 °C. The (1 1 0), (1 0 1), (2 0 0), and (2 1 1) characteristic peaks of RuO_2 phase [9] are identified from the XRD profiles. For the annealed 0.25 mmol RuO_2 films at 400–700 °C we didn't notice any RuO_2 phase through our XRD study. This could be due to formation of very thin film (below 10 nm thickness) for 0.25 mmol RuO_2 concentration due to the low viscosity of the sol solution. Simultaneously, the intensity of RuO_2 peak for all composite films increases with increasing the annealing temperature up to 600 °C. It should be noted that the peak position of RuO_2 did not shift with annealing temperature up to 600 °C. For 0.5, and 1.0 mmol RuO_2 films annealed at 700 °C, the intensity of diffraction peaks is decreased compared with 600 °C due to desorption of more RuO_3 and RuO_4 gases from the RuO_2 films at this high temperature [21, 25].

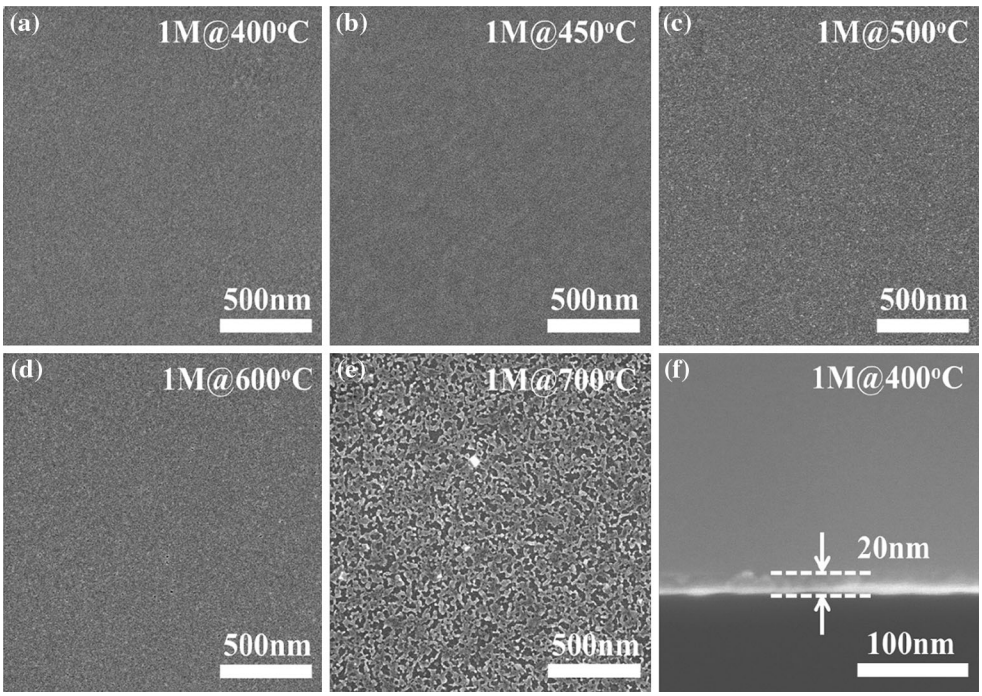

Fig. 3 SEM images of 1.0 mmol RuO_2 film annealed at **a** 400 °C, **b** 450 °C, **c** 500 °C, **d** 600 °C, and **e** 700 °C for 30 min. **f** Cross sectional view of 1.0 mmol RuO_2 film annealed at 400 °C

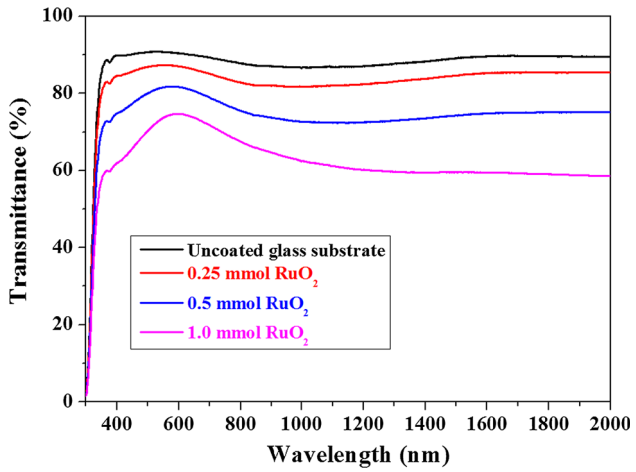

Fig. 4 The optical transmittance spectra of the samples annealed at 450 °C

The similarity of the appearance of the rutile reflections in both silicon wafers and glass substrates indicate that the physical properties of the coating, such as crystallite size and composition, were preserved independently of the substrate.

As an example, we have investigated the cross-section of the 0.25, and 0.5 mmol RuO_2 films annealed at 450 °C (not shown here) by SEM measurement. For 0.25 mmol RuO_2 film, we find it difficult to observe clear cross section of the film coated on Silicon wafer as the thickness of the film is in the range of a few nm. For 0.5 mmol RuO_2 film we measured the thickness and the value is ~13 nm. Using AFM, the topography of the sample surface can be examined. An indication of the mechanical integrity of the coating is also given by the AFM technique. Figure 2 shows the AFM images of the 0.5, and 1.0 mmol RuO_2 films annealed at 450 °C. The surface roughness values of the films evaluated from these images are 1.2, and 0.9 nm for 0.5, and 1.0 mmol RuO_2 films, respectively. Figure 3 shows the SEM images of the 1.0 mmol RuO_2 films annealed at 400–700 °C including the cross sectional view of the annealed film at 400 °C. From these images we noticed that as the annealing temperature increases from 400 to 700 °C, the surface gradually changed from smooth and denser to granular and finally porous like due to desorption of more RuO_3 and RuO_4 gaseous phases. For 1.0 mmol RuO_2 film the measured thickness value is around 20 nm. Figure 4 shows the optical transmission spectra for the 450 °C annealed samples coated on glass substrate. With the increase of Ru molar ratio the optical transparency of the films decreases in the UV–Vis-IR range. This is possibly due to the increase in the viscosity of the sol solution which subsequently results in the thicker films.

The transmittance spectra of RuO_2 films observed at wavelengths shorter than 585 nm are related to the p–d interband transitions [9]. However, the spectra at wavelengths longer than 585 nm are primarily due to free-

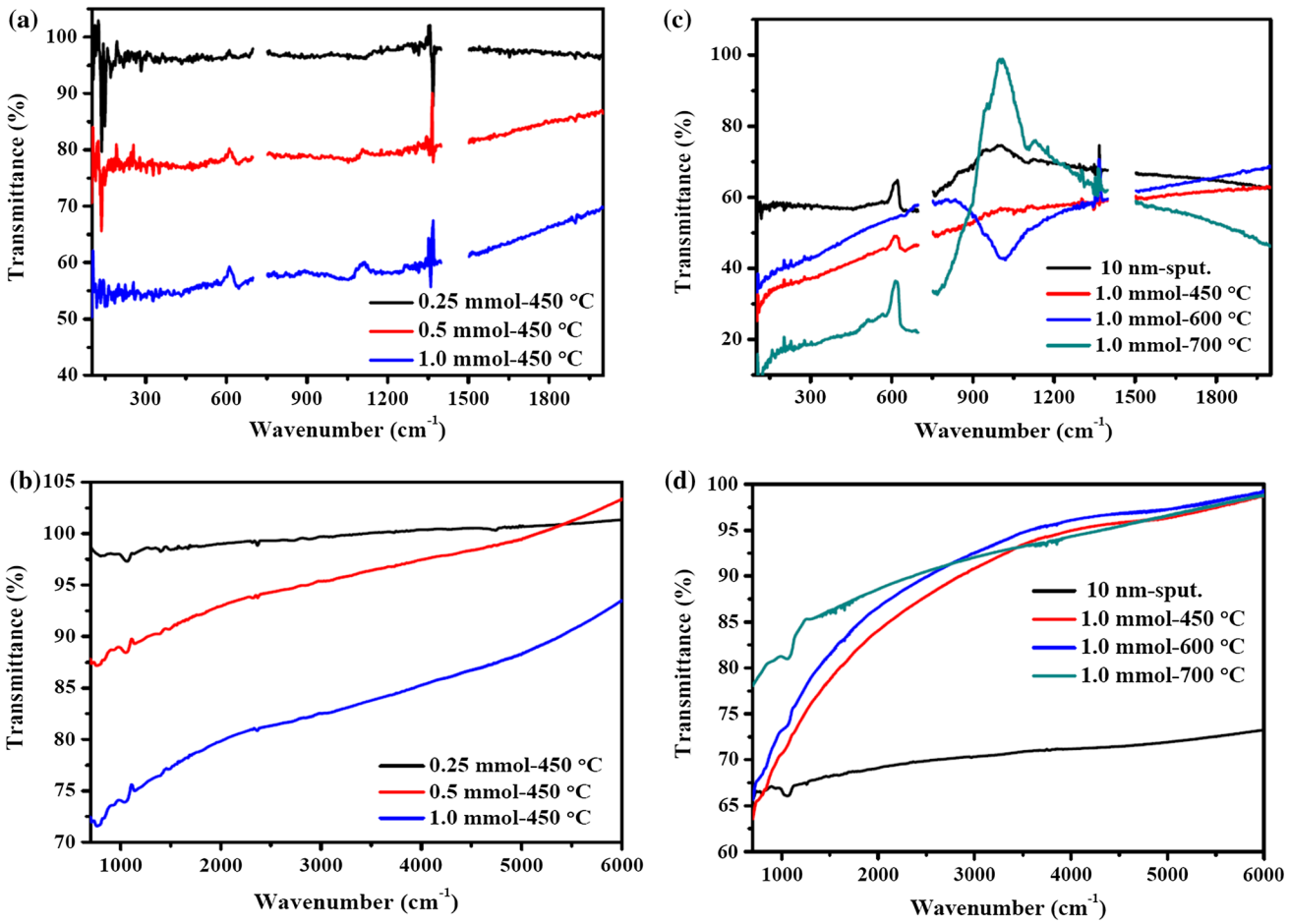

Fig. 5 FTIR spectra of some of the thin film samples

carrier absorption and d-electron intraband transitions. Figure 5a, b show the Mid-IR and Far-IR spectra of the films annealed at 450 °C; and 450, 600, and 700 °C annealed 1.0 mmol RuO_2 films (Fig. 5c, d), respectively. A vertical displacement of some of the FTIR spectra presented was necessary for easy visualization and comparison of different samples profiles. In this case, the y-axis may indicate greater than 100 % transmission for some samples. For all the films, the crystalline RuO_2 showed a main feature centered at 648 cm^{-1}. Generally for RuO_2 based thin films, two broad bands that appear at 800 and 880 cm^{-1} can be attributed to higher oxidation states of RuO_3 and RuO_4 species, respectively. These species of higher oxidation state in thin films would decompose readily and develop to thermodynamically stable RuO_2 species if left at ambient temperature [26, 27]. For our synthesized films, these 800 and 880 cm^{-1} bands from the measured FTIR spectra are not recognizable. Table 1 shows the experimental values derived from the hall measurement for 0.25, 0.5, and 1.0 mmol RuO_2 films annealed at 450 °C, using four-probe method at room temperature. The P-type conductivity of RuO_2 films is confirmed by the Hall Effect measurement. The resistivity of the RuO_2 films decreases gradually from 3.63×10^{-3} to 8.93×10^{-4} Ω cm as the RuO_2 concentration increased from 0.25 to 1.0 mmol (Table 1). We also measure the resistivity value for the 1.0 mmol RuO_2 film annealed at 600 °C and Table 2 shows the respective experimental values derived from the hall measurement for 1.0 mmol RuO_2 film. The resistivity of 1.0 mmol RuO_2 film annealed at 600 °C acquired by Hall measurement was 2.9×10^{-4} Ω cm. With the annealing temperature increment from 450 to 600 °C, carrier concentration increased from 1.92×10^{21} (1/cm^3) to 1.183×10^{22} (1/cm^3) and resistivities including sheet resistivity values are decreased for 1.0 mmol RuO_2 film. Thus for better conductivity of the synthesized sol–gel films, here concentration and annealing temperature both play a crucial role. It is well known that the conductivity depends on the carrier concentration as well as the mobility of carriers. Thus, one can say that the sol–gel process combined with the spin-coating technique provides a feasible way to fabricate RuO_2 films with

Table 1 Experimental values derived from the hall measurement for (a) 0.25 (b) 0.5, and (c) 1.0 mmol RuO_2 films annealed at 450 °C, using four-probe method

(a)	
Hall mobility (cm^2/V s)	10.1
Carrier type	P
Carrier concentration (1/cm^3)	1.71×10^{20}
Sheet carrier concentration (1/cm^2)	7.35×10^{14}
Hall coefficient (cm^3/C)	0.0365
Sheet Hall coefficient (cm^2/C)	8490
Resistivity(Ω cm)	0.00363
Sheet resistivity (Ω/sq.)	845
Hall voltage (V)	0.000004244
(b)	
Hall mobility (cm^2/V•s)	1.97
Carrier type	P
Carrier concentration (1/cm^3)	1.64×10^{21}
Sheet carrier concentration (1/cm^2)	7.05×10^{15}
Hall coefficient (cm^3/C)	0.00381
Sheet Hall coefficient (cm^2/C)	885
Resistivity(Ω cm)	0.00193
Sheet resistivity (Ω/sq.)	449
Hall voltage (V)	0.0000008852
(c)	
Hall mobility (cm^2/V s)	3.64
Carrier type	P
Carrier concentration (1/cm^3)	1.92×10^{21}
Sheet carrier concentration (1/cm^2)	8.26×10^{15}
Hall coefficient (cm^3/C)	0.00325
Sheet Hall coefficient (cm^2/C)	756
Resistivity(Ω cm)	0.000893
Sheet resistivity (Ω/sq.)	208
Hall voltage (V)	0.00000378

Table 2 Experimental values derived from the hall measurement for 1.0 mmol RuO_2 film annealed at 600 °C, using four-probe method

Hall mobility (cm^2/V s)	1.8
Carrier type	P
Carrier concentration (1/cm^3)	1.183×10^{22}
Sheet carrier concentration (1/cm^2)	2.25×10^{16}
Hall coefficient (cm^3/C)	5.3×10^{-4}
Sheet Hall coefficient (cm^2/C)	277.74
Resistivity(Ω cm)	2.9×10^{-4}
Sheet resistivity (Ω/sq.)	154.2
Hall voltage (V)	0.00013886

controlled compositions, carrier concentration, mobility, resistivity, and transmittance.

4 Conclusions

Ultrathin films of RuO_2 were wet-chemically synthesized and coated through sol–gel spin coating processes. Diffraction peaks of the RuO_2 phase are confirmed in the annealed thin films. For the 1.0 mmol RuO_2 films, as the annealing temperature increases from 400 to 700 °C, the surface gradually changed from smooth and denser to granular and finally porous like due to desorption of more RuO_3 and RuO_4 gaseous phases. The surface morphology and texture of the deposited RuO_2 films was also measured using atomic force microscopy. The resistivity of the RuO_2 films decreases gradually from 3.63×10^{-3} to 8.93×10^{-4} Ω cm as the RuO_2 concentration increased from 0.25 to 1.0 mmol. With the annealing temperature increment from 450 to 600 °C, carrier concentration increased from 1.92×10^{21} (1/cm^3) to 1.183×10^{22} (1/cm^3) and resistivities including sheet resistivity values are decreased for 1.0 mmol RuO_2 film. The fabricated film showed good electrical transport and high optical transparency together with high surface smoothness suitable for the use in organic electronics.

References

1. J.H. Son, H.K. Yu, Y.H. Song, J.-L. Lee, Electron. Mater. Lett. **4**, 157 (2008)
2. Q.X. Jia, S.G. Song, X.D. Wu, J.H. Cho, S.R. Foltyn, A.T. Findikoglu, J.L. Smith, Appl. Phys. Lett. **68**, 1069 (1996)
3. C.W. Law, K.Y. Tong, J.H. Li, K. Li, M.C. Poon, Thin Solid Films **354**, 162 (1999)
4. J.-H. Kim, D.-S. Kil, S.-J. Yeom, J.-S. Roh, N.-J. Kwak, J.-W. Kim, Appl. Phys. Lett. **91**, 052908 (2007)
5. M. Ťapajna, K. Hušeková, D. Machajdík, A.P. Kobzev, T. Schram, R. Lupták, L. Harmatha, K. Fröhlich, Microelectronic Eng. **83**, 2412 (2006)
6. S.-E. Park, H.-M. Kim, K.-B. Kim, S.-H. Min, Electrochem. Solid-State Lett. **1**, 262 (1998)
7. K. Kawano, H. Kosuge, N. Oshima, H. Funakubo, Electrochem. Solid-State Lett. **9**, C175 (2006)
8. S. Trasatti, Electrochim. Acta **36**, 225 (1991)
9. J.-S. Jeng, Y.-T. Lin, J.S. Chen, Thin Solid Films **518**, 5416 (2010)
10. H. Over, Chem. Rev. **112**, 3356 (2012)

11. L.-J. Meng, V. Teixeira, M.P. dos Santos, Thin Solid Films **442**, 93 (2003)
12. J.H. Lim, D.J. Choi, W.I. Cho, Y.S. Yoon, J. Korean Phys. Soc. **39**, S382 (2001)
13. C.L. Cheng, Y.F. Chen, R.S. Chen, Y.S. Huang, Appl. Phys. Lett. **86**, 103104 (2005)
14. J. Si, S.B. Desu, J. Mater. Res. **8**, 2644 (1993)
15. X. Fang, M. Tachiki, and T. Kobayashi, Deposition and properties of PLD grown RuO_2 thin film, Proceedings of SPIE 3175, Third International Conference on Thin Film Physics and Applications, 331 **(1998)**; doi:10.1117/12.300697
16. I. Zhitomirsky, L. Gal-Or, Mater. Lett. **31**, 155 (1997)
17. C.-C. Hu, K.-H. Chang, Electrochim. Acta **45**, 2685 (2000)
18. T. Aaltonen, P. Alén, M. Ritala, M. Leskelä, Chem. Vap. Dep. **9**, 45 (2003)
19. K.E. Swider-Lyons, C.T. Love, D.R. Rolison, J. Electrochem. Soc. **152**, C158 (2005)
20. V.K. Tagirov, D.M. Chizhikov, E.K. Kazenas, L.K. Shubochkin, Zhurnal Neorganicheskoj Khimii **20**, 2035 (1975)
21. L. Armelao, D. Barreca, B. Moraru, J. Non-Cryst, Solids **316**, 364 (2003)
22. A.G. Emslie, F.T. Bonner, L.G. Peck, J. Appl. Phys. **29**, 858 (1958)
23. C. Hummelgård, J. Gustavsson, A. Cornell, H. Olin, J. Bäckström, Thin Solid Films **536**, 74 (2013)
24. J.H. Yi, P. Thomas, M. Manier, J.P. Mercurio, J. Phys. IV France **8**, Pr9-45 (1998)
25. K.S. Kim, N. Winograd, J. Catal. **35**, 66 (1974)
26. H.Y.H. Chan, C.G. Takoudis, M.J. Weaver, J. Catal. **172**, 336 (1997)
27. S.K. Park, R. Kanjolia, J. Anthis, R. Odedra, N. Boag, L. Wielunski, Y.J. Chabal, Chem. Mater. **22**, 4867 (2010)